A Framework Based on Determining Feasible Transaction Regions (FTRs) for P2P Trading of Energy Communities in an Active Distribution Network Using ADMM Method

Mohammad Sedaghat[1], Esmaeel Rokrok[1,*] and Meysam Doostizadeh[1]

[1] *Faculty of Electrical Engineering, University of Lorestan, Khorramabad, Iran*
**Corresponding author: Rokrok.e@lu.ac.ir*

Manuscript received 11 August, 2025; revised 1 February, 2026; accepted 2 May, 2026. Paper no. JEMT-2508-1568.

The growth of distributed generation resources, local electricity markets, and peer-to-peer energy exchanges has introduced challenges, notably balancing network technical constraints with maximum utilization of distributed generation units. Static operation envelopes (SOEs) and Dynamic operation envelopes (DOEs) have emerged as solutions, statically and dynamically setting network constraints over time, respectively. However, these envelopes often calculated by distribution system operators (DSOs) and imposed on users, may overlook participants' preferences, reducing profits and incentives to engage in local markets. Addressing this, the paper proposes a framework for determining feasible transaction regions (FTRs), established through agreements between energy communities (ECs) and DSOs. These FTRs represent optimal operating envelopes that consider uncertainties in ECs and DSO constraints. The framework models EC uncertainties using the chance constraint method and solves the optimization problem with the alternating direction method of multipliers (ADMM) on a standard IEEE 69-bus network using GAMS software. Results highlight the method's efficiency and accuracy compared to DOE and SOE approaches, effectively defining safe regions for peer-to-peer energy trading in distribution networks. This novel approach optimizes energy exchanges while respecting technical constraints and participant preferences. Also, this paper, by providing different confidence levels during simulations, verifies the proper efficiency of the proposed method in operating the uncertainty of distributed generations. The simulation results show cost reduction of ECs and loss reduction in the distribution network along with increment in active and reactive power exchanges compared to DOE and SOE methods.

Keywords: *Energy communities, dynamic operation envelopes, peer-to-peer energy trading, feasible transaction region, and active distribution network.*

http://dx.doi.org/10.22109/jemt.2026.539980.1568

Nomenclature

Acronyms

P2P	Peer-to-Peer
DSO	Distribution System Operator
SOE	Static Operational Envelope
EC	Energy Community
ADMM	Alternating Direction Method of Multipliers
DOE	Dynamic Operational Envelope
FTR	Feasible Transaction Region

Sets and Indices

i,j	Index for network bus
C, C'	Index for set of energy communities
EC, EC'	Index for energy communities
t	Index for time interval
$*$	Indicator of optimal value
f	Index for flexible load
u	Index for dispatchable unit
v	Index for Non-dispatchable loads
s	Index for energy storage
$\sim$	Indicator of proposed value of shared variable

EC's decision variables

$Q_{u,t}^{D}$	Reactive power of dispatchable unit u of the EC
$Q_{f,t}^{FL}$	Reactive power of flexible load f in the EC
Q_{t}^{EX}	Reactive power exchange with the distribution network
P_{t}^{Total}	Total active power injected by the EC

Q_t^{Total}	Total reactive power, injected by the EC
$P_{s,t}^{ch/dch}$	Charging/Discharging power of storage s in the EC
$P_{c,t}^{inj}$	Total real injected power
$P_{u,t}^{D}$	Active power of dispatchable unit u in the EC
$P_{u,t}^{ND}$	Active power of non-dispatchable unit v in the EC
$P_{f,t}^{FL}$	Active power of flexible load f in the EC
$P_{s,t}^{Bat}$	Active net power of storage s in the EC
P_t^{EX}	Active power exchanged with the distribution network
$E_{s,t}^{Bat}$	State-of-charge of the storage s in the EC
$Q_{c,t}^{inj}$	Total reactive injected power

DSO's decision variables

$\tilde{P}_{nd,t}^{ND,EC}$	Predicted output power of the non-dispatchable unit
$P_{k,i,j,t}^{line} / Q_{k,i,j,t}^{line} / S_{k,i,j,t}^{line}$	Active/reactive/apparent power flowing through the line (i,j), under operating condition k
$\ddot{P}_{i,t}^{DSO} / \ddot{Q}_{i,t}^{DSO}$	Upper bound of active/reactive FTR, at bus i
$\underset{\cdot\cdot}{P}_{i,t}^{DSO} / \underset{\cdot\cdot}{Q}_{i,t}^{DSO}$	Lower bound of active/reactive FTR, at bus i
$Q_{c,c',t}^{tr}, Q_{c',c,t}^{tr}$	Reactive power negotiated in p2p trades
$\tilde{Q}_{c,t}, \underset{\sim}{Q}_{c,t}$	Upper and lower limits of ECs reactive power
$\tilde{P}_{c,t}, \underset{\sim}{P}_{c,t}$	Upper and lower limits of ECs real power
$\tilde{P}_{i,t}^{DSO}, \underset{\sim}{P}_{c,t}^{DSO}$	Upper and lower limits of DSO real power
$U_{k,i,t}$	Squared voltage magnitude of bus i at hour t, under operating condition k
$J_{k,i,j,t}^{line}$	Squared current flowing through the line *(i,j)*, under operating condition k
$P_{k,t}^{ref} / Q_{k,t}^{ref}$	Active/reactive power imported to the network
$P_{c,c',t}^{tr}, P_{c',c,t}^{tr}$	Real power negotiated in p2p trades
$\underline{U}_i, \overline{U}_i$	Lower and upper limit of bus voltage

Parameters

R_u^D	Maximum ramp rate limit of dispatchable unit u
$\bar{P}_{v,t}^{ND} / P_{v,t}^{avg}$	Rated capacity/average power of non-dispatchable unit v
$\underline{P}_f^{FL} / \bar{P}_f^{FL}$	Active power limits of flexible load f
$P_{f,t}^{FL,Des}$	Desired consumption value of flexible load f
pf_f	Power factor of flexible load f
E_f^{min}	Minimum required energy of flexible load f
R_f^{FL}	Maximum ramp rate limit of flexible load f
$\underline{P}_s^{dch} / \bar{P}_s^{dch}$	Discharging power limits of storage s
$\underline{E}_s / \bar{E}_s$	Stored energy limits of storage s
$\underline{\Delta}_t^P / \bar{\Delta}_t^P$	Uncertainty envelopes of ECs
ε	Stopping criterion in the ADMM algorithm
δ	Confidence level
$r_{i,j}$, $x_{i,j}$	Resistance and reactance between buses i and j
$\gamma_{u,t}^D$	Marginal cost of dispatchable unit u
$\gamma_{v,t}^{ND}$	Deviation cost coefficient of non-dispatchable v
$\gamma_{f,t}^{FL}$	Deviation cost coefficient of flexible load v
$\gamma_{s,t}^{Deg}$	Degradation cost coefficient storage s
γ_t^{ex}	Hourly energy price in distribution network
$\underline{P}_u^D / \bar{P}_u^D$	Active power limits of dispatchable unit u
$\underline{Q}_u^D / \bar{Q}_u^D$	Reactive power limits of dispatchable unit u
$\underline{P}_s^{ch} / \bar{P}_s^{ch}$	Charging power limits of storage s
$\eta_s^{ch} / \eta_s^{dch}$	Charging/discharging efficiency of storage s
$\bar{P}^{EX}$	Maximum active power exchanged with the distribution network
IN_c^i	Bus-community incident matrix element: 1 if EC c is located at bus i, 0 otherwise
$\boldsymbol{\rho}, \theta$	Penalty factors in the ADMM algorithm
$, \underset{\sim}{\pi}_{c,t}^{p}\ \tilde{\pi}_{c,t}^{Q}, \tilde{\pi}_{c,t}^{p}$	Lagrange coefficients
$\underset{\sim}{\pi}_{c,t}^{Q}, \tilde{\alpha}_{i,t}, \underset{\sim}{\alpha}_{i,t}, \tilde{\beta}_{i,t}, \underset{\sim}{\beta}_{i,t}$	

1. Introduction

The development of distributed generation resources has led to widespread changes in energy trading in distributed networks. One of these developments is the growth of local energy markets. The local energy market is a platform for trading locally generated (renewable) energy between small-scale subscribers in a geographically and socially close community. [1] Distributed generation resources are managed within the framework of local energy markets in distribution networks, and producers and consumers of renewable energy can actively participate in the market through energy exchanges and local electricity markets. Local energy markets offer numerous benefits, including reducing losses, facilitating energy transmission, and promoting the development of a smart grid [2].

With the growth of local electricity markets, the development and implementation of microgrids [3] and energy communities (ECs) in the distribution network have also expanded significantly. Microgrids and ECs connected to distribution networks consist of renewable resources such as solar cells, wind turbines, electric vehicles [4], fixed

and flexible loads, etc. These communities increase the flexibility, stability, and resilience of the network and also perform peak shaving in the distribution system [5]. Despite providing many advantages, the presence of microgrids and ECs has also created challenges, such as modeling renewable resources due to their inherent complexity [6], including electric vehicles and energy storage systems [7], load forecasting [8], energy management [9], and flexibility, as well as implementing network technical constraints. These challenges have provided the basis for various research studies. In this study, the aspect of how to implement network technical constraints during ECs' transactions in the distribution network is discussed.

In local energy markets, peer-to-peer energy exchanges are an emerging and effective method that brings several benefits, including independence and security for users, helping to increase the participation of small-scale producers in local electricity markets, and enhancing grid stability. Peer-to-peer energy trades enable network consumers to exchange their surplus energy production with each other without intermediaries and under the distribution network. The development of peer-to-peer exchanges encourages small-scale consumers to use distributed generation and participate in local electricity markets [10].

However, the decisions of producers and consumers participating in the market may not be operable in the physical distribution network, and the network operator faces technical challenges in implementing the agreements made on the distribution network platform. These challenges include maintaining voltage and line loading within the permitted range, establishing fairness among all traders in terms of equal opportunity for energy supply and demand, and also considering the private security of peer-to-peer exchanges. In recent years, researchers have proposed various solutions to address the challenges raised, which have led to the development of the security and volume of peer-to-peer energy exchanges in distributed networks. However, a comprehensive method that covers all the aforementioned challenges is still one of the goals of energy researchers.

In the operation of distribution networks with the presence of independent entities such as energy communities (ECs) that include a set of distributed generation units[11], the more the operation is in the form of ownership and control, the less the ECs are willing to participate and establish peer-to-peer exchanges in local electricity markets. As a result, if the operation is directed towards regulation, the participation and encouragement of ECs in local electricity markets will increase. Therefore, the transition of the operator from ownership to the regulator is one of the new and modern aspects in the field of energy markets. In general, the role of the operator and independent entities as market players in energy exchanges in distribution networks can be classified into three categories:

In the first category, the market is completely in the hands of the operator, for example, the distribution system operator (DSO). In such a way that the agreements of independent entities and ECs with each other on the volume and price of energy in the local market are made available to the DSO, and the operator approves or rejects the agreements based on the physical conditions of the network and technical constraints. Therefore, many peer agreements are not realized. In this case, the network constraints are maintained by the ownership of the DSO.

For example, in [12], the DSO receives and checks the P2P transactions of the prosumers, performs network sensitivity analysis, and eliminates transactions that may compromise the integrity of the network. In [13], the authors propose an electrical distance-based peer-to-peer transaction matching mechanism that prioritizes transactions from those prosumers those are physically close to each other to reduce line overload. However, due to the dependence of these approaches on the DSO, concerns about the privacy of transaction information are raised, and the incentive for generators-consumers to participate in local electricity markets is reduced.

The authors [14,15] present a decentralized peer-to-peer trading mechanism in which consumers select their peers for energy exchange by assigning indices based on the cost of network usage, the electrical distance of generators, and power exchange losses. However, these approaches rely on DSO to directly manage peer-to-peer transactions and, despite considering technical constraints and decentralization, conflict with the privacy of ECs' trade information.

In the second category, the system operator establishes its desired technical constraints through a negotiation mechanism. This agreement is on the amount of energy injection or absorption by ECs. In [16], the distribution network constraints are established through a negotiation mechanism and agreement on the amount of energy export and import. The drawback of this method is the lack of justice in the network operator's negotiations with ECs because in this method, the amount of ECs' participation in exchanges depends greatly on their location. For example, independent entities and ECs located at the end buses of distribution networks, which are generally radial, have restrictions on energy consumption.

Also, in another set of studies [17,18], the optimal allocation of transactions in local electricity markets is carried out by imposing a network usage fee, the basis of calculation of which for market prosumers is the distributed local marginal price (DLMP). The drawback of this method is the allocation of a marginal price to all prosumers at each stage of peer-to-peer negotiations, which challenges the condition of independence of participants. In addition, simultaneous marginal price changes in peer-to-peer transactions cannot be applied in this type of pricing.

The third category is the consideration of static and dynamic operating limits for market players. In recent research, in a simple and preliminary way, static operation envelopes (SOEs) are considered to maintain the technical constraints of the network [19]. This, despite maintaining the network constraints during peer-to-peer energy exchanges, causes ECs to be unable to use their full energy capacity, which reduces the flexibility of the network.

In the latest mechanism for implementing network constraints in the third category, dynamic operating envelopes (DOEs) have been proposed. These envelopes, which are calculated by the DSO and communicated to the ECs, dynamically determine the scope of energy exchange and the establishment of exchanges between ECs. In this case, in addition to maintaining network constraints, the volume of energy exchanges of market players also increases. [20].

Initially, the DOE method only considered the exchange of consumers with the network and the injection of energy into the upstream network. However, with the development of peer-to-peer exchanges, this method has been applied in recent research in modeling based on P2P trades. [21].

The authors in [22] proposed that the full observation and awareness of EC constraints by DSO to calculate DOEs. In this way, the uncertainty of ECs was considered in the DOE calculation. This ignores the privacy of end users and, in turn, causes less incentive for ECs to participate in local electricity markets. Also, all data of ECs is not available to DSO.

Reference [23] proposes a framework in which DOEs are integrated into peer-to-peer trades. In this approach, the DSO calculates dynamic operation envelopes after receiving the DOEs desired by the ECs, and then P2P trades are formed. In this case, although DOEs are calculated based on the preferences of the ECS, the problem is that the ECs do not have the opportunity to adjust their P2P trades based on the final allocation of DOEs, and it may not lead to the best interests of the ECs.

In the recent studies on the optimal calculation of DOEs, reference [24] has calculated the operating envelopes in agreement with DSO, which covers the weaknesses of previous studies, but it is still necessary to implement an integrated framework that considers the uncertainty of distributed generation resources in DOE modeling.

From the study of the above research, two important issues are identified as gaps in conventional methods.

First, in general, the uncertainty of energy production sources leads to dependence on the flexibility market, so that if this is not taken into account in the transactions, in some cases the network operator needs the flexibility market to maintain technical constraints, and consequently, costs arise for the network and ECs. As a result, it becomes difficult for the network operator and ECs to carry out accurate planning.

The second is to protect the privacy of ECs and DSO while encouraging energy communities to participate in the local electricity market and P2P energy trades. Traditionally, to accurately implement technical constraints in the network, either the DSO must be aware of the production and uncertainties of the ECs or the energy communities must be aware of the preferences and constraints of the DSO, which in the first case reduces the incentive for ECs to participate in P2P markets due to concerns about their privacy, and in the second case, it is impossible to provide network operator information to ECs. As a result, it is necessary to provide a safe margin so that the privacy of ECs and DSO is preserved.

Also, an important limitation of existing DOE-based frameworks is the assumption that DOEs are determined solely by the DSO. While this centralization ensures technical compliance, it may limit EC flexibility. To address these issues, this study introduces a framework for calculating feasible transaction regions (FTRs) based on collaborative agreements between DSOs and ECs. This approach incorporates uncertainties and preferences specific to ECs, allowing for more equitable and efficient participation in local electricity markets.

In this paper, in order to provide a comprehensive and coherent framework for determining the optimal network operation limits using the maximum capacity of ECs, feasible transaction regions (FTRs) are introduced. This framework is obtained by integrating the role of independent network actors in categories 2 and 3, namely the negotiation mechanism and dynamic operation envelopes. In this way, operation envelopes are calculated using negotiation between ECs and DSO and provide the FTRs.

In this framework, DSO provides its desired operation envelopes according to the technical constraints of the network, and on the other hand, ECs provide their desired operation constraints and their energy production and absorption limits according to the uncertainty of their inherent production resources. In this situation, the agreement reached, which is introduced in the form of FTRs, takes into account both the technical constraints of the network and the uncertainties of ECs. As a result, the challenges of the failure to realize the pre-planning of independent entities and the need for a flexible market are minimized and energy efficiency is increased. This situation increases the security of users' information and their motivation to participate in the local electricity market. Also, in the proposed method, the uncertainty of ECs is calculated by the chance constraint method and numerical simulation based on different confidence levels is implemented to prove the accuracy of the proposed method in modeling uncertain resources. The determination of the FTRs according to the proposed method is calculated by an optimization method based on the ADMM algorithm. In order to provide a comprehensive comparison among dynamic operating envelope (DOE), static operating envelope (SOE), and proposed feasible transaction region (FTR) methods, table 1 is presented.

Table 1. Comparison of the proposed method with other methods for calculating operating limits in peer-to-peer energy transactions

Ref.	Network Constraints	Operation Constraints Implementation	Uncertainty Impacts of ECs
[13]	Centralized	-	-
[17]	Decentralized	-	-
[19]	SOE	By DSO	-
[20]-[22]	DOE	By DSO	-
[24]	DOE	Agreement between ECs and DSO	-
Proposed method	FTR	Agreement between ECs and DSO	✓

Given the independent nature of ECs, their private data is not shared with the network operator. Consequently, the dynamic operational envelopes (DOEs) calculated by the network operator, even if they guarantee the secure operation of the grid, suffer from two fundamental shortcomings. First, they do not account for the uncertainties inherent to the ECs. Second, they do not ensure the satisfaction of all consumers and may be contested by some market participants.

This paper designs a decentralized framework to address these two issues. In the proposed framework, the distribution system operator (DSO) participates in the local market alongside the ECs, but not for the purpose of buying or selling energy from them. Instead, the DSO engages in the market to determine the operational envelopes in coordination with the ECs. As a result, ECs—by leveraging their own forecasts of renewable resource uncertainties—can influence the operational envelopes. By expanding these envelopes, they increase their own flexibility and freedom of action, enabling them to develop more effective strategies in the market. Therefore, in addition to negotiating active and reactive power exchanges among themselves, the ECs also negotiate with the DSO regarding the minimum and maximum permissible power injections into the grid. Furthermore, since the operational envelopes are established with the participation of the ECs, no EC can subsequently dispute them. This approach ensures complete transparency and reduces the DSO's role from a direct controller—which can limit competition in local markets—to that of a regulator. Accordingly, the contributions of the proposed method can be summarized as follows:

1- In this study, a decentralized framework based on P2P trades of energy communities (ECs) consisting of solar and wind generation, fixed and flexible loads, and batteries in the active distribution network is presented. In order to maintain the distribution network constraints and increase the volume of exchanges, an optimal area called the feasible transaction region (FTR) has been determined, which, in addition to maintaining the technical constraints of the network, leads to an increase in the volume of peer-to-peer exchanges of ECs in the distribution network by determining the maximum permissible operating ranges. FTR is calculated from the agreement between ECs and DSO. In this way, the preferences of ECs are also taken into account in calculating the operating limits.

2- A safe margin for the uncertainty of distributed generation resources located in ECs is also considered so that during exchanges, despite the uncertainty of the resources, we do not go beyond the proposed operating limits. In this case, no data is shared between ECs and DSO, and the operation area is obtained while the DSO is not aware of the wind and PV generation of ECs. This is while the calculated operation limits in recent studies have generally not taken this point into account.

3- In general, the uncertainty of energy production sources leads to dependence on the flexibility market, so that if this is not taken into

account in exchanges, in some cases DSO needs the flexibility market to maintain technical constraints, and consequently, costs arise for the network and ECs. As a result, it becomes difficult for DSO and ECs to carry out accurate planning. This is while, by considering uncertainty in the proposal method, transactions are settled without the need for the flexibility market.

4- In this research, in order to verify and demonstrate the effect of the uncertainty of distributed generation sources, different confidence levels have been considered for distributed generation sources located in ECs. Also, the optimization of ECs' P2P trades is carried out with the ADMM algorithm, which is a robust and effective method for solving problems with many variables.

The remainder of this paper is structured as follows: Section 2 delves into the framework description developed to enhance participant benefits in local electricity markets and P2P trades based on proposed FTR method. Section 3 explores the problem formulation for both participants and DSOs, along with the modeling of FTRs. Section 4 explains the ADMM method in detail for optimizing the objective function. Section 5 presents the simulation results derived from applying this framework to a test system. Finally, Section 6 offers conclusions drawn from the study's findings.

2. Framework Description

This section starts with an in-depth discussion of the idea of FTRs. Next, it clarifies the functions of prosumers, ECs, and the DSO in the suggested methodology, concluding with an explanation of the general framework.

2.1. Feasible Transaction Regions (FTRs)

As mentioned earlier, in most studies, DOEs are calculated by the DSO and assigned to the ECs, or it is assumed that the DSO has full knowledge of the uncertainties of ECs and calculates the optimal dynamic operating envelopes based on it. The drawback of this scheme is that the notified DOEs may conflict with the ECs' purchased flexibility. However, if DOEs are calculated by agreement between ECs and DSOs and taking into account the uncertain nature of ECs and their flexibility, more accurate values for DOEs are calculated, and the profit margin of ECs is also increased.

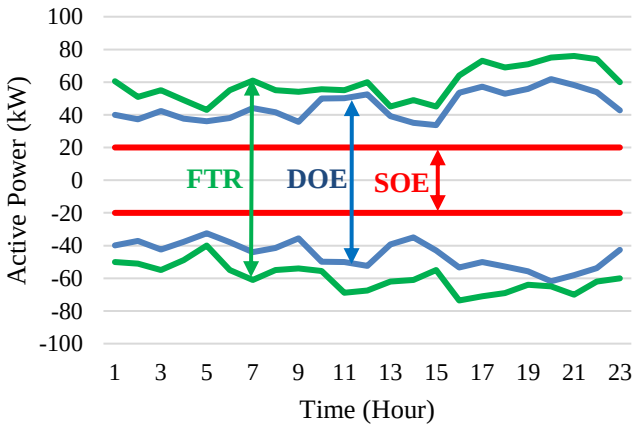

Fig. 1. FTR compared to dynamic operational envelopes (DOEs) and static operational envelopes (SOEs).

Therefore, in this paper, we calculate the feasible transaction regions for ECs based on the technical constraints of the network and the preferences of communities. Figure 1 shows feasible transaction regions according to the proposed method compared to the DOEs and SOEs calculated by DSO for a sample EC.

In order to provide a comprehensive comparison among dynamic operating envelope (DOE), static operating envelope (SOE), and proposed feasible transaction region (FTR) methods, table 2 is presented.

2.2. P2P Energy Transaction Considering FTR Method

In this paper, energy communities consist of photovoltaic systems, wind turbines, energy storage devices, and both fixed and flexible loads. Their goal is to optimize individual advantages while adhering to operational limitations.

Another important role in P2P trading is played by DSO, which is responsible for calculating the feasible transaction regions in agreement with ECs. The system operator's goal is to minimize the cost of operating the distribution network according to the power injection pattern associated with the allocation of FTRs, as well as maintaining the technical constraints of the network. In this paper, it is assumed that DSO does not know the amount of P2P transactions and their prices.

For example, the P2P energy trading of 3 ECs in a distribution network, considering the feasible transaction regions, is shown in Figure 2. As can be seen in Figure 2, ECs perform P2P energy trading with each other and with the upstream network. To determine the feasible transaction regions, ECs first determine their uncertainties in each time interval based on their calculated uncertainty value. DSO also calculates the desired permitted operating region in each time interval based on the allowed network limits and the maximization of the network operating region. Then, the final feasible transaction regions are calculated from the agreement between DSO and ECs for each time interval. To explain the proposed framework and describe the proposed scheme step by step, the following points are necessary:

- In this paper, P2P energy trades are performed between energy communities in an active distribution network. An energy community (EC) consists of a wind turbine, solar cells, fixed and flexible loads, and batteries.
- ECs establish P2P energy trades to minimize costs and achieve the most economically feasible transaction regions, taking into account their inherent uncertainties.
- The DSO aims to maintain the technical limitations of the ADN and maximize the allowed region of power injection by ECs to increase its flexibility in network operation.
- According to the proposed framework, each EC makes the best decision about the upper and lower limits of its required operating region by examining the data related to its estimated energy production pattern. DSO also determines the upper and lower permissible operating limits. Then, the feasible transaction regions are calculated from the agreement between the ECs and DSO.
- The market type in the proposed framework is assumed to be day-ahead, and the actors (DSO and ECs) reach an agreement through a cooperative game to calculate the feasible transaction regions.
- The constraints of the equations are relaxed using the ADMM algorithm and placed in the objective functions, and the market variables are calculated using the Nash equilibrium theory.

Table 2. Comparison of operational envelope frameworks

Feature	SOE [19]	DOE [20]-[22]	FTR [Proposed framework]
Temporal Resolution	Fixed for the entire optimization horizon.	Time-varying (updated per interval, e.g., hourly).	Time-varying & negotiated per interval.
Primary DSO Focus	Worst-case security based on a single snapshot.	Security with updated snapshots over time.	Secure & optimal flexibility via market signals.
Uncertainty Handling	Implicit (via conservative, fixed assumptions).	Limited to updated point forecasts.	Explicit & Proactive via ECs' private forecasts influencing the region.
EC Participation Mode	Passive recipient of fixed limits.	Passive recipient of updated, DSO-calculated limits.	Active Co-creator in a distributed negotiation.
Information Privacy	Protected (ECs share no data).	Compromised (may require sharing forecast data).	Fully Protected (only boundary proposals are exchanged).

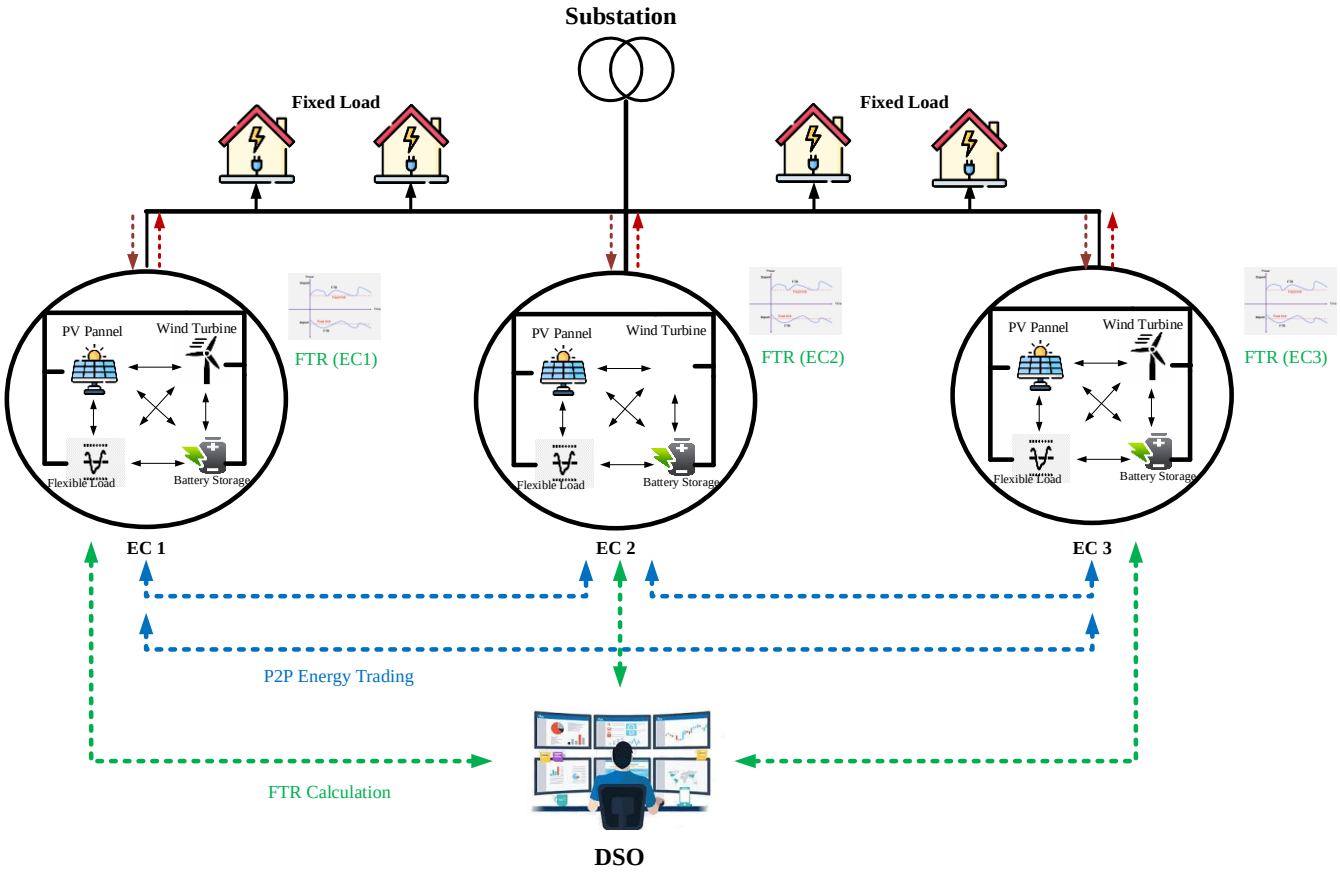

Fig. 2. Peer-to-peer energy trading between 3 ECs, with the calculation of FTR negotiated with DSO

3. Mathematical Formulation

The proposed mechanism involves independent Energy Communities (ECs) optimizing their internal operations and desired energy trades. Since ECs act autonomously, a negotiation process is required to agree on exchange amounts. The Distribution System Operator (DSO) seeks to establish grid power limits in agreement with the ECs, not unilaterally. This structure forms a cooperative game, where participants collaborate for a mutually beneficial outcome. To find a solution that is both optimal and acceptable to all, a Nash equilibrium—where no participant benefits from changing their strategy—is pursued. This section presents each participant's optimization problem and the process for reaching this market equilibrium.

3.1. The EC Local Problem Formulation

In equation (1), the objective function of ECs is presented to minimize production costs, which consists of six terms. In this

equation, $t \in T$ represents each one-hour time interval and represents [15].

$$\begin{aligned} min\ J_c = & \underbrace{\sum_{u,t} \gamma_{u,t}^{D} . P_{u,t}^{D,EC}}_{Term1} + \\ & \underbrace{\sum_{v,t} \gamma_{v,t}^{ND} . (P_{v,t}^{ND,EC} - \tilde{P}_{v,t}^{ND,EC})^2}_{Term2} + \\ & \underbrace{\sum_{f,t} \gamma_{f,t}^{FL} . (P_{f,t}^{FL,EC} - \tilde{P}_{f,t}^{FL,EC})^2}_{Term3} \\ & + \underbrace{\sum_{s,t} \gamma_{s,t}^{Deg} . P_{s,t}^{Bat,EC}}_{Term4} + \\ & \underbrace{\left[\begin{array}{l} \left(\sum_t -\left(\tilde{P}_{EC,t} - \underset{\sim}{P}_{EC,t} \right) + \omega \left(\tilde{P}_{EC,t} - \underset{\sim}{P}_{EC,t} \right)^2 \right) \\ + \left(\sum_t -\left(\tilde{Q}_{EC,t} - \underset{\sim}{Q}_{EC,t} \right) + \omega \left(\tilde{Q}_{EC,t} - \underset{\sim}{Q}_{EC,t} \right)^2 \right) \end{array} \right]}_{Term5} \\ & + \underbrace{\sum_t \gamma_t^{ex} . P_t^{EC,ex}}_{Term6} \end{aligned} \quad (1)$$

In equation (1), $\gamma_{u,t}^{D}$ is the marginal cost of the dispatchable unit *u* in hour *t* for each *EC* and $P_{u,t}^{D,EC}$ represents the actual power generated by the dispatchable unit *u* in hour *t*. $\gamma_{v,t}^{ND}$ is the cost coefficient of the deviation from the predicted output value of the non-dispatchable unit *v* and $P_{v,t}^{ND,EC}$ indicates the actual power output value of the non-dispatchable unit *nd* at hour *t*. $\tilde{P}_{v,t}^{ND,EC}$ is also the amount of power output predicted by the non-dispatchable units at hour *t*. $\gamma_{f,t}^{F}$ is the discomfort cost of the flexible load *f* at hour *t*. $P_{f,t}^{FL,EC}$ is the actual power consumption of the flexible load *f* at time *t*. Also, $\tilde{P}_{f,t}^{FL,EC}$ is the planned power consumption of the flexible load *f* at time *t*. $\gamma_{s,t}^{Deg}$ is the battery degradation cost at time *t* and $P_{s,t}^{Bat,EC}$ is the battery output power of each *EC* at time *t*. The fifth term of equation (1) is related to the calculation of feasible transaction regions considering the uncertainty of each EC at time t. The purpose of establishing this term is to increase the regions between the high and low operational envelopes of the real and reactive power of ECs. The larger this area, the more capable the ECs are of providing the flexibility needed to overcome uncertainties. This increases the feasible transaction regions [26]. It should be noted that the quadratic term with the coefficient *ω* is intended to distribute the flexibility ranges equally over different periods and control the variance of feasible transaction regions.

The sixth term shows the objective function of the cost of energy exchange between ECs and the distribution network. In this term, γ_t^{ex} is the energy price of the upstream network (time of use) and $P_t^{EC,ex}$ is the real power exchanged between ECs and the distribution network. Equations (2) to (15) express the constraints of the ECs' optimization problem.

$$\underset{\sim}{P}_u^{D,EC} \le P_{u,t}^{D,EC} \le \bar{P}_u^{D,EC} \quad (2)$$

$$\underset{\sim}{Q}_u^{D} \le Q_{u,t}^{D,EC} \le \bar{Q}_u^{D} \quad (3)$$

$$-P_u^R \le P_{u,t}^{D,EC} - P_{u,t-1}^{D,EC} \le P_u^R \qquad \forall u,t>1 \quad (4)$$

$$0 \le P_{v,t}^{ND,EC} \le \bar{P}_{v,t}^{ND,EC} \quad (5)$$

$$\underset{\sim}{P}_f^{FL} \le P_{f,t}^{FL,EC} \le \bar{P}_f^{FL} \quad (6)$$

$$Q_{f,t}^{FL,EC} = P_{f,t}^{FL,EC} \sqrt{1-pf_f^{\,2}} \,/\, pf_f \quad (7)$$

$$\sum_t P_{f,t}^{FL,EC} \ge E_f^{min} \quad \forall f \in FL \quad (8)$$

$$-P_f^R \le P_{f,t}^{FL,EC} - P_{f,t-1}^{FL,EC} \le P_f^R \quad (9)$$

$$P_{s,t}^{Bat,EC} = P_{s,t}^{dch} - P_{s,t}^{ch} \quad \forall s \in S \quad (10)$$

$$\underset{\sim}{P}_s^{ch} \le P_{s,t}^{ch} \le \bar{P}_s^{ch} \quad (11)$$

$$\underset{\sim}{P}_s^{dch} \le P_{s,t}^{dch} \le \bar{P}_s^{dch} \quad (12)$$

$$E_{s,t} = E_{s,t-1} + \eta_s^{ch} . P_{s,t}^{ch} - \frac{P_{s,t}^{dch}}{\eta_s^{dch}} \quad (13)$$

$$\underset{\sim}{E}_s \le E_{s,t} \le \bar{E}_s \quad (14)$$

$$0 \le P_t^{EC,ex} \le \bar{P}^{EC,ex} \quad (15)$$

$$\begin{aligned} P_t^{Total,EC} = & \sum_u P_{u,t}^{D,EC} + \sum_v P_{v,t}^{ND,EC} + \sum_s P_{s,t}^{Bat,EC} \\ & + P_t^{EC,ex} - \sum_f P_{f,t}^{FL,EC} \end{aligned} \quad (16)$$

$$Q_t^{Total,EC} = \sum_u Q_{u,t}^{D,EC} + Q_t^{EC,ex} - \sum_f Q_{f,t}^{FL,EC} \quad (17)$$

$$\underset{\sim}{P}_t^{EC,tot} \le P_t^{EC,tot} \le \tilde{P}_t^{EC,tot} \quad (18)$$

$$\underset{\sim}{Q}_t^{EC,tot} \le Q_t^{EC,tot} \le \tilde{Q}_t^{EC,tot} \quad (19)$$

$$\underset{\sim}{P}_t^{EC} \le \underset{\sim}{\Delta}^P \quad (20)$$

$$\bar{\Delta}_t^P \le \tilde{P}_t^{EC,p} \quad (21)$$

Equations (2) and (3) represent the lower and upper limits of real and reactive power of the dispatchable unit *u*, respectively. The lower and upper ramps of the real power of the dispatchable unit *u* are determined by the constraint of equation (4). The planned power limits of the non-dispatchable unit *v* are also determined by equation (5). Equation (6) specifies the lower and upper limits of the real power, and constraint (7) specifies the relationship between the active and reactive powers of the flexible load *f*, which are assumed to have a constant power factor in this study, for each EC. Equation (8) shows the minimum energy consumption of the flexible loads. Equation (9) determines the lower and upper ramps of the real power changes of flexible loads. Equation (10) models the battery power of each EC at time t. Equations (11) and (12) express the charge and discharge ranges of the batteries. Equation (13) shows how to calculate the energy at each time t. In equation (13), η_s^{ch} and η_s^{dch} are the efficiency coefficients of charging and discharging of batteries, respectively. Equation (14) specifies the permissible range of energy stored in

batteries. The limit of real power purchased by ECs from the upstream network is presented in equation (15). Equations (16) and (17) represent the total real and reactive power of the ECs at time t, respectively. Equations (18) and (19) show the upper and lower limits of the real and reactive power of the ECs based on their estimated uncertainty. In equation (20), the lower bound of the feasible transaction region is expressed as a lower bound of the uncertainty of ECs, which must be greater than or equal to the lower bound of the uncertainty of ECs. Similarly, in equation (21), the upper bound of the feasible transaction region is expressed as a lower bound of the uncertainty of the energy communities. These two constraints are intuitively shown in Figure 1.

After mathematical modeling of each energy community, the P2P trades model and the agreement of each EC with DSO are presented in equations (22)-(32). In equation (22), $P_{c,t}^{inj}$ is the real injected power of all ECs at time t, which is calculated from the sum of the real power of dispatchable, non- dispatchable and battery loads minus the flexible real power of all ECs. In equation (23), $Q_{c,t}^{inj}$ is the reactive injected power of all ECs at time *t* [20].

$$\sum_{\substack{u\in D\\ t\in T}} P_{u,t}^{D,EC} + \sum_{\substack{v\in ND\\ t\in T}} P_{v,t}^{ND,EC} + \sum_{s\in S} P_{s,t}^{Bat,EC} - \sum_{\substack{f\in FL\\ t\in T}} P_{f,t}^{FL,C} = P_{c,t}^{inj} \tag{22}$$

$$\sum_{u} Q_{u,t}^{D,EC} - \sum_{f} Q_{f,t}^{FL,EC} = Q_{c,t}^{inj} \tag{23}$$

$$P_{EC,t}^{inj} = \sum_{EC'\in C'} P_{EC,EC',t}^{tr} \tag{24}$$

$$P_{c,c',t}^{tr} + P_{c',c,t}^{tr} = 0 \quad :(\lambda_{c,c',t}) \tag{25}$$

$$Q_{c,c',t}^{tr} + Q_{c',c,t}^{tr} = 0 \quad :(\mu_{c,c',t}) \tag{26}$$

In equation (24), EC' denotes the energy community in the neighborhood of EC that exchanges energy with each other with the abbreviation *tr*. The exchanged injected power is calculated from equation (24). According to equations (25) and (26), the real and reactive power traded between each EC and EC' at time t have the agreed price $\lambda_{c,c',t}$ and $\mu_{c,c',t}$, respectively. These powers must be equal. In equation (25), $P_{c,c',t}^{tr}$ and $P_{c',c,t}^{tr}$ are respectively the real powers agreed upon in the P2P trading between *EC* and EC' at time *t*, and in equation (26), $Q_{c,c',t}^{tr}$ and $Q_{c',c,t}^{tr}$ are respectively the reactive powers agreed upon in the P2P trading between the *EC* and EC' at time *t*. In these equations, $EC \in c$ and $EC' \in c'$.

$$\underset{\sim}{P}_{c,t} \le P_{c,t}^{inj} \le \tilde{P}_{c,t} \tag{27}$$

$$\underset{\sim}{Q}_{c,t} \le Q_{c,t}^{inj} \le \tilde{Q}_{c,t} \tag{28}$$

$$\tilde{P}_{c,t} = \tilde{P}_{i,t}^{DSO} . IN_{c}^{i} \quad :(\tilde{\pi}_{c,t}^{p}) \tag{29}$$

$$\underset{\sim}{P}_{c,t} = \underset{\sim}{P}_{i,t}^{DSO} . IN_{c}^{i} \quad :(\underset{\sim}{\pi}_{c,t}^{p}) \tag{30}$$

$$\tilde{Q}_{c,t} = \tilde{Q}_{i,t}^{DSO} . IN_{c}^{i} \quad :(\tilde{\pi}_{c,t}^{Q}) \tag{31}$$

$$\underset{\sim}{Q}_{c,t} = \underset{\sim}{Q}_{i,t}^{DSO} . IN_{c}^{i} \quad :(\underset{\sim}{\pi}_{c,t}^{Q}) \tag{32}$$

Equations (27) and (28) show the permissible range of real and reactive powers injected by each EC at time *t*. These ranges are the feasible transaction regions (FTRs) that must be obtained from the agreement with the DSO. Equations (29) to (32) show the calculation of FTRs. In this paper, the optimization problem is solved with the ADMM algorithm, which is fully explained in Section 4. This algorithm has Lagrangian coefficients for optimization. In calculating the FTRs with the corresponding Lagrangian coefficients of the ADMM algorithm, $\tilde{\pi}_{c,t}^{p}$ and $\underset{\sim}{\pi}_{c,t}^{p}$ are the corresponding Lagrangian coefficients of the EC and DSO agreement on the upper and lower limits of real power. Also, $\tilde{\pi}_{c,t}^{Q}$ and $\underset{\sim}{\pi}_{c,t}^{Q}$ are the corresponding Lagrangian coefficients for the upper and lower limits of reactive power, respectively. $\tilde{P}_{i,t}^{DSO}$ and $\underset{\sim}{P}_{c,t}^{DSO}$ are respectively the upper and lower limits of real power. Also, $\tilde{Q}_{i,t}^{DSO}$ and $\underset{\sim}{Q}_{i,t}^{DSO}$ are the upper and lower limits of reactive power respectively desired by DSO in order to maintain the technical constraints of the network. IN_{c}^{i} is also the internal matrix that determines the connection of ECs to distribution network nodes.

In this paper, the chance constraint method is used to calculate feasible transaction regions. In this method, the power generation by non-dispatchable units (solar and wind) varies around the predicted values.

$$P_r\left\{P_{v,t}^{ND} \le \bar{P}_{v}^{ND}\right\} \ge \delta \tag{33}$$

$$P_r\left\{P_{v,t}^{ND} \ge \underset{\sim}{P}_{v}^{ND}\right\} \ge \delta \tag{34}$$

In equations (33) and (34), the desired confidence level of the ECs is shown by δ. To convert the above chance constraints into definite constraints, reference [26] is used. According to this reference, $\bar{P}_{v}^{ND}$ and $\underset{\sim}{P}_{v}^{ND}$ are calculated by through the inverse of the cumulative function and using equations (35) and (36).

$$\bar{P}_{v}^{ND} = \left(\psi^{ND}\right)^{-1}(\delta) \tag{35}$$

$$\underset{\sim}{P}_{v}^{ND} = \left(\psi^{ND}\right)^{-1}(1-\delta) \tag{36}$$

In this study, the normal distribution function is used to model the uncertainty of non-dispatchable units, and the inverse cumulative function in the normal distribution is calculated by equation (37) to determine the minimum and maximum values of $P_{v,t}^{ND}$.

$$\left(\psi^{ND}\right)^{-1}(\delta) = e + \frac{\delta\sqrt{3}}{\pi}\ln\frac{\delta}{1-\delta} \tag{37}$$

In this way, the predicted region of output power from non-renewable units ($P_{nd,t}^{ND}$) is calculated from equation (38):

$$\underset{\sim}{P}_{v,t}^{ND} = P_{v,t}^{avg} - \frac{\delta_{v,t}^{ND}\sqrt{3}}{\pi}\ln\left(\frac{\delta}{1-\delta}\right) \le P_{v,t}^{ND} \le P_{v,t}^{avg} + \frac{\delta_{v,t}^{ND}\sqrt{3}}{\pi}\ln\left(\frac{\delta}{1-\delta}\right) = \bar{P}_{v,t}^{ND} \tag{38}$$

Since different energy production sources are present in ECs, a mechanism must be provided in which the FTRs that are the result of the upper and lower limits of the resources available in the ECs are calculated. For this purpose, two sets of variables corresponding to the power of each of the resources available in the ECs are considered, which represent the upper and lower limits of the power of the

resources available in the ECs. These variables are represented as $\ddot{\mathbf{X}}$ and $\underset{\leftrightarrow}{\mathbf{X}}$, which represent the upper and lower bounds of the vector x in equation (39), respectively. Finally, vector $\mathbf{X}$ represents the decision variables of ECs. With this description, feasible transaction regions are calculated from equation (40):

$$\mathbf{X}=\begin{bmatrix} P_{u,t}^{D,EC}, Q_{u,t}^{D,EC}, P_{v,t}^{ND}, P_{f,t}^{FL,C}, Q_{f,t}^{FL,C} \\ , P_{s,t}^{ch}, P_{s,t}^{dch}, P_{s,t}^{Bat,EC}, E_{s,t}, P_{t}^{EC,ex}, Q_{t}^{EC,ex} \end{bmatrix} \tag{39}$$

$$\begin{aligned}\mathbf{\Gamma}=&\left[\underset{\sim}{P}_{u,t}^{D,EC}, \tilde{P}_{u,t}^{D,EC}\right]\times\left[\underset{\sim}{Q}_{u,t}^{D,EC}, \tilde{Q}_{u,t}^{D,EC}\right]\times\ldots \\ &\times\left[\underset{\sim}{Q}_{t}^{EC,ex}, \tilde{Q}_{t}^{EC,ex}\right]\end{aligned} \tag{40}$$

In equation (40), $\mathbf{\Gamma}$ is the feasible transaction region and is calculated from the product of the upper and lower bounds of the decision variables of ECs. The energy communities should expand the space $\mathbf{\Gamma}$ as much as possible. For this purpose, the vector of variables $\ddot{\mathbf{X}}$ and $\underset{\leftrightarrow}{\mathbf{X}}$ must satisfy equations (2) to (15). Also, the equations (41) to (60) must be hold for these variables:

$$\underset{\sim}{P}_{u,t}^{D,EC} \le P_{u,t}^{D,EC} \le \tilde{P}_{u,t}^{D,EC} \tag{41}$$

$$\underset{\_}{P}_{u,t}^{D,EC} \le \underset{\sim}{P}_{u,t}^{D,EC} \le P_{u,t}^{D,EC} \le \tilde{P}_{u,t}^{D,EC} \le \bar{P}_{u,t}^{D,EC} \tag{42}$$

$$\underset{\sim}{Q}_{u,t}^{D,EC} \le Q_{u,t}^{D,EC} \le \tilde{Q}_{u,t}^{D,EC} \tag{43}$$

$$\underset{\_}{Q}_{u,t}^{D,EC} \le \underset{\sim}{Q}_{u,t}^{D,EC} \le Q_{u,t}^{D,EC} \le \tilde{Q}_{u,t}^{D,EC} \le \bar{Q}_{u,t}^{D,EC} \tag{44}$$

$$\underset{\sim}{P}_{v,t}^{ND,EC} \le P_{v,t}^{ND,EC} \le \tilde{P}_{v,t}^{ND,EC} \tag{45}$$

$$\underset{\_}{P}_{v,t}^{ND,EC} \le \underset{\sim}{P}_{v,t}^{ND,EC} \le P_{v,t}^{ND,EC} \le \tilde{P}_{v,t}^{ND,EC} \le \bar{P}_{v,t}^{ND,EC} \tag{46}$$

$$\underset{\sim}{Q}_{v,t}^{ND,EC} \le Q_{v,t}^{ND,EC} \le \tilde{Q}_{v,t}^{ND,EC} \tag{47}$$

$$\underset{\_}{Q}_{v,t}^{ND,EC} \le \underset{\sim}{Q}_{v,t}^{ND,EC} \le Q_{v,t}^{ND,EC} \le \tilde{Q}_{v,t}^{ND,EC} \le \bar{Q}_{v,t}^{ND,EC} \tag{48}$$

$$\underset{\sim}{P}_{f,t}^{FL,EC} \le P_{f,t}^{FL,EC} \le \tilde{P}_{f,t}^{FL,EC} \tag{49}$$

$$\underset{\_}{P}_{F,t}^{FL,EC} \le \underset{\sim}{P}_{f,t}^{FL,EC} \le P_{f,t}^{FL,EC} \le \tilde{P}_{f,t}^{FL,EC} \le \bar{P}_{f,t}^{FL,EC} \tag{50}$$

$$\underset{\sim}{Q}_{f,t}^{FL,EC} \le Q_{f,t}^{FL,EC} \le \tilde{Q}_{f,t}^{FL,EC} \tag{51}$$

$$\underset{\_}{Q}_{f,t}^{FL,EC} \le \underset{\sim}{Q}_{f,t}^{FL,EC} \le Q_{f,t}^{FL,EC} \le \tilde{Q}_{f,t}^{FL,EC} \le \bar{Q}_{f,t}^{FL,EC} \tag{52}$$

$$\underset{\sim}{P}_{s,t}^{Bat,EC} \le P_{s,t}^{Bat,EC} \le \tilde{P}_{s,t}^{Bat,EC} \tag{53}$$

$$\underset{\_}{P}_{s,t}^{Bat,EC} \le \underset{\sim}{P}_{s,t}^{Bat,EC} \le P_{s,t}^{Bat,EC} \le \tilde{P}_{s,t}^{Bat,EC} \le \bar{P}_{s,t}^{Bat,EC} \tag{54}$$

$$\underset{\sim}{Q}_{s,t}^{Bat,EC} \le Q_{s,t}^{Bat,EC} \le \tilde{Q}_{s,t}^{Bat,EC} \tag{55}$$

$$\underset{\_}{Q}_{s,t}^{Bat,EC} \le \underset{\sim}{Q}_{s,t}^{Bat,EC} \le Q_{s,t}^{Bat,EC} \le \tilde{Q}_{s,t}^{Bat,EC} \le \bar{Q}_{s,t}^{Bat,EC} \tag{56}$$

$$\underset{\sim}{P}_{t}^{EC,ex} \le P_{t}^{EC,ex} \le \tilde{P}_{t}^{EC,ex} \tag{57}$$

$$\underset{\_}{P}_{t}^{EC,ex} \le \underset{\sim}{P}_{t}^{EC,ex} \le P_{t}^{EC,ex} \le \tilde{P}_{t}^{EC,ex} \le \bar{P}_{t}^{EC,ex} \tag{58}$$

$$\underset{\sim}{Q}_{t}^{EC,ex} \le Q_{t}^{EC,ex} \le \tilde{Q}_{t}^{EC,ex} \tag{59}$$

$$\underset{\_}{Q}_{t}^{EC,ex} \le \underset{\sim}{Q}_{t}^{EC,ex} \le Q_{t}^{EC,ex} \le \tilde{Q}_{t}^{EC,ex} \le \bar{Q}_{t}^{EC,ex} \tag{60}$$

So, the upper and lower envelopes of the real power of feasible transaction regions are calculated from equations (61) and (62), respectively, and the upper and lower envelopes of the reactive power of feasible transaction regions are calculated from equations (63) and (64), respectively.

$$\begin{aligned}\overline{FTR}_{t}^{EC,P} =& \sum_{u}\tilde{P}_{u,t}^{D,EC} + \sum_{nd}\tilde{P}_{v,t}^{ND,EC} + \sum_{s}\tilde{P}_{s,t}^{Bat,EC} \\ &+\tilde{P}_{t}^{EC,ex} - \sum_{f}\underset{\sim}{P}_{f,t}^{FL,EC}\end{aligned} \tag{61}$$

$$\begin{aligned}\underline{FTR}_{t}^{EC,P} =& \sum_{d}\underset{\_}{P}_{u,t}^{D,EC} + \sum_{nd}\underset{\_}{P}_{v,t}^{ND,EC} + \sum_{s}\underset{\_}{P}_{s,t}^{Bat,EC} \\ &+\underset{\_}{P}_{t}^{EC,ex} - \sum_{fl}\tilde{P}_{f,t}^{FL,EC}\end{aligned} \tag{62}$$

$$\begin{aligned}\overline{FTR}_{t}^{EC,Q} =& \sum_{d}\tilde{Q}_{u,t}^{D,EC} + \sum_{nd}\tilde{Q}_{v,t}^{ND,EC} + \sum_{s}\tilde{Q}_{s,t}^{Bat,EC} \\ &+\tilde{Q}_{t}^{EC,ex} - \sum_{fl}Q_{f,t}^{FL,EC}\end{aligned} \tag{63}$$

$$\begin{aligned}\underline{FTR}_{t}^{EC,Q} =& \sum_{d}\underset{\sim}{Q}_{u,t}^{D,EC} + \sum_{nd}\underset{\sim}{Q}_{v,t}^{ND,EC} + \sum_{s}\underset{\sim}{Q}_{s,t}^{Bat,EC} \\ &+\underset{\sim}{Q}_{t}^{EC,ex} - \sum_{fl}\tilde{Q}_{f,t}^{FL,EC}\end{aligned} \tag{64}$$

3.2. DSO's Local Problem Formulation

In this sub-section, the equations related to calculating the objective function of DSO are presented

Also, the amount of the FTRs desired by DSO which is calculated from the agreement with the ECs, is evaluated to adjust the permissible range of network operation and fulfill the technical constraints. In equation (65), *i* represents the network buses and Ω shows the scenario. Equation (65) represents the objective function of DSO with the aim of maximizing the range of real and reactive powers of the network for more flexible operation while maintaining network integrity.

$$Max \sum_{i\in\Omega_{tr}}\left[\left(\ddot{P}_{i,t}^{DSO} - \underset{\leftrightarrow}{P}_{i,t}^{DSO}\right)+\left(\ddot{Q}_{i,t}^{DSO} - \underset{\leftrightarrow}{Q}_{i,t}^{DSO}\right)\right] \tag{65}$$

In equation (65), $\ddot{P}_{i,t}^{DSO}$ and $\underset{\leftrightarrow}{P}_{i,t}^{DSO}$ respectively represent the upper and lower limits of the real power desired by DSO at time *t* in bus *i*. Also, $\ddot{Q}_{i,t}^{DSO}$ and $\underset{\leftrightarrow}{Q}_{i,t}^{DSO}$ respectively represent the upper and lower limits of the reactive power desired by DSO at time *t* in bus *i*. In the following, equations (66) to (72) represent the constraints of DSO equations.

$$\begin{aligned}&U_{k,i,t} - U_{k,j,t} = 2(P_{k,i,j,t}^{line}.r_{i,j} + Q_{k,i,j,t}^{line}.x_{i,j}) \\ &-J_{k,i,j,t}^{line}.Z_{i,j}^{2}\end{aligned} \tag{66}$$

$$J_{k,i,j,t}^{line}.U_{k,i,t} \ge {P_{k,i,j,t}^{line}}^{2} + {Q_{k,i,j,t}^{line}}^{2} \tag{67}$$

$$\underline{U}_{i} \le U_{k,i,t} \le \bar{U}_{i} \tag{68}$$

$${P_{k,i,j,t}^{line}}^{2} + {Q_{k,i,j,t}^{line}}^{2} \le \bar{S}_{i,j,t} \tag{69}$$

$$U_{k,i=1,t} = V_{ref}^{2} \tag{70}$$

$$P_{k,i,t}^{DSO} + P_{k,i=1,t}^{ref} + P_{k,i,j,t}^{line} - r_{j,i}.J_{k,i,j,t}^{line} - P_{k,i,j,t}^{line} = 0 \tag{71}$$

$$Q^{DSO}_{k,i,t} + Q^{ref}_{k,i=1,t} + Q^{line}_{k,i,j,t} - x_{j,i}.J^{line}_{k,i,j,t} - Q^{line}_{k,i,j,t} = 0 \quad (72)$$

Equations (66) and (67) represent the voltage balance. *k* is the operating mode counter (upper or lower envelope of the FTRs) and $U_{k,i,t}$ is the voltage of bus i at time *t*. Also, $U_{k,j,t}$ is the voltage of bus *j* at time *t*. $P^{line}_{k,i,j,t}$ is the real power flowing between buses *i* and *j* at time *t* and $Q^{line}_{k,i,j,t}$ is the reactive power flowing between buses *i* and *j* at time *t*. Also, $r_{i,j}$ and $x_{i,j}$ are the resistance and reactance between buses *i* and *j* respectively. *Z* is the branch impedance between buses *i* and *j*. In equation (68) $\underline{U}_i$ and $\overline{U}_i$ represent the lower and upper limits of voltage in each bus *i*, respectively. In equation (69), $P^{line\ 2}_{k,i,j,t}$, $Q^{line\ 2}_{k,i,j,t}$ and $\overline{S}_{i,j,t}$ represent the square of real power, the square of reactive power and the upper limit of power between buses *i* and *j* in each negotiation round at time *t*, respectively. In equation (70), $U_{k,i=1,t}$ is the reference voltage at the first bus at time *t*. Equations (71) and (72) represent the balance of the distribution network operator's real and reactive powers between buses *i* and *j* in each negotiation round at time *t* in comparison with the corresponding reference values.

$$\overleftrightarrow{P}^{DSO}_{i,t} = \tilde{P}_{c,t}.IN^{i}_{c} \quad (\tilde{\alpha}_{i,t}) \quad (73)$$

$$\underset{\sim}{\overleftrightarrow{P}}^{DSO}_{i,t} = \underset{\sim}{P}_{c,t}.IN^{i}_{c} \quad (\underset{\sim}{\alpha}_{i,t}) \quad (74)$$

$$\overleftrightarrow{Q}^{DSO}_{i,t} = \tilde{Q}_{c,t}.IN^{i}_{c} \quad (\tilde{\beta}_{i,t}) \quad (75)$$

$$\underset{\sim}{\overleftrightarrow{Q}}^{DSO}_{i,t} = \underset{\sim}{Q}_{c,t}.IN^{i}_{c} \quad (\underset{\sim}{\beta}_{i,t}) \quad (76)$$

Like equations (29) to (32) in subsection 3.1 which are presented to calculate FTRs with the agreement between ECs and DSO, according to equations (73) to (76), the minimum and maximum ranges of the real and reactive powers desired by DSO must be calculated with the agreement of the ECs. In this case, the Lagrangian coefficients of the ADMM algorithm are $\tilde{\alpha}_{i,t}$ and $\underset{\sim}{\alpha}_{i,t}$ for the upper and lower limits of real power, respectively. Also, $\tilde{\beta}_{i,t}$ and $\underset{\sim}{\beta}_{i,t}$ are the upper and lower limits of reactive power, respectively. $\tilde{P}_{c,t}$ and $\underset{\sim}{P}_{c,t}$ are the upper and lower limits of real power, respectively. Also $\tilde{Q}_{c,t}$ and $\underset{\sim}{Q}_{c,t}$ are respectively the upper and lower limits of reactive power of each EC, which are presented for agreement with DSO.

3.3. Unified Distributed Optimization Problem

As formulated in Sections 3.1 and 3.2, the ECs and the DSO have their respective local optimization problems. The challenge is to solve these problems coordinately, considering their interdependence

$$Min \sum_{c} \mathcal{F}^{EC}_{c}(\mathbf{x}_c) - \mathcal{G}^{DSO}(\mathbf{y}) \quad (77)$$

Subject to:

$$\mathcal{H}^{EC}_{c}(\mathbf{x}_c) \le \mathbf{0}; \quad \forall c \quad (78)$$

$$\mathcal{R}^{DSO}(\mathbf{y}) \le 0 \quad (79)$$

$$\mathcal{A}.\mathbf{x}_c + \mathcal{B}.\mathbf{x}_{c'} = \mathbf{0} \quad :(\boldsymbol{\lambda}_{c,c'}); \forall c, c' \quad (80)$$

$$\mathcal{M}.\mathbf{x}_c + \mathcal{N}.\mathbf{y} = \mathbf{0} \quad :(\boldsymbol{\mu}_c); \forall c \quad (81)$$

The overall market objective function is given in (77). Its first term represents the sum of the ECs' costs, and its second term expresses the distance between FTRs, which is to be maximized and therefore appears with a negative sign in the objective function. In this objective, $\mathbf{x}_c$ is the vector of decision variables for the c'th community, and $\mathbf{y}$ is the vector of decision variables for the DSO.

The internal operational constraints for each EC's resources are expressed in (78), and the internal operational constraints for the distribution network are given in (79).

The agreement among ECs on the amount of active and reactive power exchange is generally stated in (80). In this equation, the EC c reaches an agreement with the EC c' on how much active and reactive power to exchange. The vector $\boldsymbol{\lambda}_{c,c'}$ is the dual multiplier of this constraint and is interpreted as the trading price.

The agreement between ECs and the DSO on the FTR values is formulated in (81), with the dual multiplier vector of $\boldsymbol{\mu}_c$. In this reformulation, the functions (e.g. $\mathcal{F}^{EC}_{c}$, $\mathcal{G}^{DSO}$, $\mathcal{H}^{EC}_{c}$, $\mathcal{R}^{DSO}$) and the matrices (e.g. $\mathcal{A}$, $\mathcal{B}$, $\mathcal{M}$, $\mathcal{N}$) are derived from the underlying technical and economic characteristics of the system.

3.4. ADMM Reformulation

Two fundamental challenges in this optimization problem motivate the use of the ADMM algorithm for its decentralized solution. The first motivation is to preserve the autonomy of the market participants (ECs and the DSO) without requiring a central market operator with access to all data. The second motivation is that EC costs are in dollars, while the DSO's objective is in per-unit (pu), making them dimensionally incompatible for direct summation. Therefore, the use of distributed algorithms like ADMM is essential [27].

It is evident that the problem (77)-(81) is separable. If constraints (80) and (81) were not considered in this optimization problem, each market participant could solve its own problem independently. It is precisely these two constraints that link the optimization problems of the participants. Consequently, they are relaxed using the ADMM technique. The relaxed form of the ECs' problem is given in (82) and (84), where $\boldsymbol{\rho}$ is the penalty coefficient in the ADMM algorithm.

$$\begin{aligned} &Min\ \mathcal{F}^{EC}_{c}(\mathbf{x}_c) \\ &+\sum_{c'}\left[\boldsymbol{\lambda}_{c,c'}\left(\mathcal{A}.\mathbf{x}_c + \mathcal{B}.\tilde{\mathbf{x}}_{c'}\right) + \frac{1}{2}\left\|\boldsymbol{\rho}\odot\left(\mathcal{A}.\mathbf{x}_c + \mathcal{B}.\tilde{\mathbf{x}}_{c'}\right)\right\|^2_2\right] \\ &+\boldsymbol{\mu}^{EC}_{c}\left(\mathcal{M}.\mathbf{x}_c + \mathcal{N}.\tilde{\mathbf{y}}\right) + \frac{1}{2}\theta\left\|\mathcal{M}.\mathbf{x}_c + \mathcal{N}.\tilde{\mathbf{y}}\right\|^2_2 \end{aligned} \quad (82)$$

$$\mathcal{H}^{EC}_{c}(\mathbf{x}_c) \le \mathbf{0}; \quad \forall c \quad (83)$$

Where the vector $\boldsymbol{\rho}$ and parameter θ denote the ADMM's penalty factors and $\odot$ represents the elementwise product. The relation (82) presents the objective function of the optimization problem for community c. It is important to note that since the community c does not have direct access to the decision variables of c' or the DSO, it substitutes these variables with the values proposed by community c' and the DSO, respectively, within its local optimization. Consequently, in this reformulation, the tilded vectors (e.g. $\tilde{\mathbf{x}}_{c'}$ and $\tilde{\mathbf{y}}$) are treated as input parameters. Similarly, the relaxed form of the DSO's problem is given in (84) and (85), where θ is the ADMM penalty coefficient.

$$Min \ -\mathcal{G}^{DSO}\left(\mathbf{y}\right)+\boldsymbol{\mu}_c^{DSO}\left(\mathcal{M}.\tilde{\mathbf{x}}_c+\mathcal{N}.\mathbf{y}\right) +\frac{1}{2}\theta\left\|\mathcal{M}.\tilde{\mathbf{x}}_c+\mathcal{N}.\mathbf{y}\right\|_2^2 \quad (84)$$

$$\mathcal{R}^{DSO}\left(\mathbf{y}\right)\le 0 \quad (85)$$

It is essential to note that the parameters $\boldsymbol{\mu}_c^{EC}$ and $\boldsymbol{\mu}_c^{DSO}$ are, in fact, the same as the dual multiplier $\boldsymbol{\mu}_c$, but used locally on the EC and DSO sides, respectively.

4. Solution Methodology

To clarify the proposed algorithm, the solution algorithm is described in detail in this section and a flowchart along with a pseudocode network have been provided to enhance comprehensibility.

In this section, the proposed algorithm for reaching an agreement between the ECs and the DSO on energy transactions and the FTRs is elaborated. Given the convergence capability of the Alternating Direction Method of Multipliers (ADMM), this algorithm is employed to solve the problem. The overall procedure is illustrated in Figure 3. As outlined in this algorithm, the market participants—namely the ECs and the DSO—first cooperatively initialize the penalty parameters for the ADMM algorithm. For instance, they jointly determine the vector $\boldsymbol{\rho}$ and parameter θ. It is important to note that if the ECs were to initialize different values for these parameters prior to executing the algorithm, convergence would still be achieved. However, the agreed-upon prices between them, which are updated according to Equations (86) - (88), would differ, consequently leading to the cancellation of the transactions [26].

$$\boldsymbol{\lambda}_{c,c'}^{new}=\boldsymbol{\lambda}_{c,c'}^{old}+\boldsymbol{\rho}\odot\left(\mathcal{A}.\tilde{\mathbf{x}}_c+\mathcal{B}.\tilde{\mathbf{x}}_{c'}\right) \quad (86)$$

$$\boldsymbol{\mu}_c^{EC,new}=\boldsymbol{\mu}_c^{EC,old}+\theta\left(\mathcal{M}.\tilde{\mathbf{x}}_c+\mathcal{N}.\tilde{\mathbf{y}}\right) \quad (87)$$

$$\boldsymbol{\mu}_c^{DSO,new}=\boldsymbol{\mu}_c^{DSO,old}+\theta\left(\mathcal{M}.\tilde{\mathbf{x}}_c+\mathcal{N}.\tilde{\mathbf{y}}\right) \quad (88)$$

Therefore, the penalty parameters must be adopted uniformly among all ECs. Furthermore, to initiate the iterations of the ADMM algorithm, the shared variables among all participants—i.e., all tilded variables—must be initialized. For this purpose, all participants can set the initial values for these shared variables to zero as their starting proposal.

In the next step, each EC proceeds to solve its own optimization problem. After solving its local problem, each EC shares its updated shared variables with the other market participants to facilitate the next iteration. Naturally, the DSO must wait until it has received all shared variables from the ECs before it can proceed to solve its own optimization problem.

In the third step, the DSO solves its optimization problem and subsequently shares its own set of shared variable values. Once all market participants have solved their respective optimization problems and exchanged the shared variables, the Lagrangian multipliers are updated, and the algorithm's stopping criteria (89)-(90) are checked. It is important to note that since the penalty parameters are considered equal among all market participants, the values of the primal and dual residuals will be identical on both sides of any negotiation.

$$\left\|\mathcal{A}.\tilde{\mathbf{x}}_c+\mathcal{B}.\tilde{\mathbf{x}}_{c'}\right\|_2^2\le\varepsilon,\ \left\|\mathcal{M}.\tilde{\mathbf{x}}_c+\mathcal{N}.\tilde{\mathbf{y}}\right\|_2^2\le\varepsilon \quad (89)$$

$$\left\|\boldsymbol{\lambda}_{c,c'}^{new}-\boldsymbol{\lambda}_{c,c'}^{old}\right\|_2^2\le\varepsilon,\ \left\|\boldsymbol{\mu}_c^{EC,new}-\boldsymbol{\mu}_c^{EC,old}\right\|_2^2\le\varepsilon, \left\|\boldsymbol{\mu}_c^{DSO,new}-\boldsymbol{\mu}_c^{DSO,old}\right\|_2^2\le\varepsilon \quad (90)$$

Consequently, if the stopping criteria are satisfied, the algorithm terminates, and the necessary schedules for the following day are determined. To ensure maximum clarity, this entire procedure is presented in Pseudocode 1.

Pseudocode 1: Decentralized framework for P2P energy trading and FTR scheduling

Initialize: $\boldsymbol{\lambda}_{c,c'}$, $\boldsymbol{\mu}_c^{EC}$, $\boldsymbol{\mu}_c^{DSO}$, $\boldsymbol{\rho}$, θ, and ε

While: Stopping criteria (89)-(90) are not met: **do**
ECs minimize (82), subjected to (83)
DSO minimizes (84), subjected to (85)
Each market participant updates the respected Lagrangian multipliers using (86)-(88)
End while

The flowchart for solving the feasible transaction region calculation problem is shown in Figure 3. According to this figure, the problem-solving process is carried out in the following way: first, the parameters are initialized, then the agreement problem between ECs is solved, and its output is used to solve the DSO problem. If the convergence condition is met, the problem-solving process ends. Otherwise, the coefficients of the problem-solving algorithm are updated, and the optimization and problem-solving process is started again with the new problem-solving coefficients until the convergence condition is achieved.

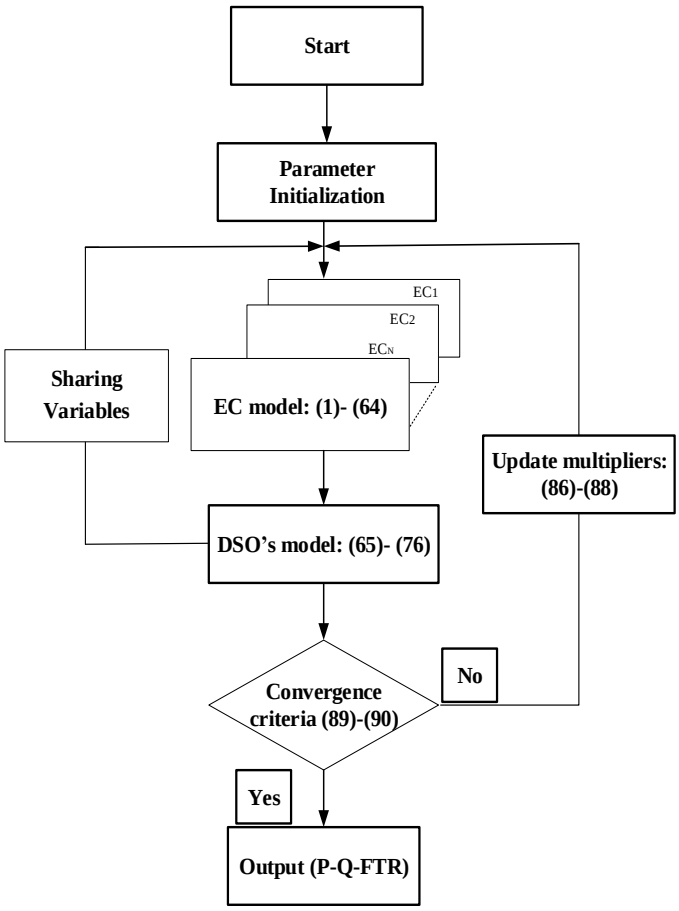

Fig. 3. Flowchart of the proposed FTR method

5. Numerical Results

5.1. Description of the studied system and initial simulation of the proposed method

In this section, the 69-bus distribution network [29] is considered to implement the proposed method, as shown in Figure 5. In this study, the base power for per-unit calculations is assumed to be 100 kW. According to Figure 5, five ECs are connected to the network. To ensure the comprehensiveness of the simulations, all these ECs are equipped with flexible loads, dispatchable and non-dispatchable energy sources, and energy storage systems. The generation capacity of the non-dispatchable unit for EC3 is as shown in Figure 4.

The forecasted generation of the other ECs is a proportional share of the forecasted power of the ECs. In this study, the generation capacity of EC1 is 0.14 times that of the EC3. Similarly, these ratios for EC2, EC4, and EC5 are 0.326, 0.279, and 0.259, respectively. Other technical and economic specifications of the ECs are provided in Tables 3 and 4, respectively [17]. Also, all the sets, parameters and variables are explained in Nomenclature.

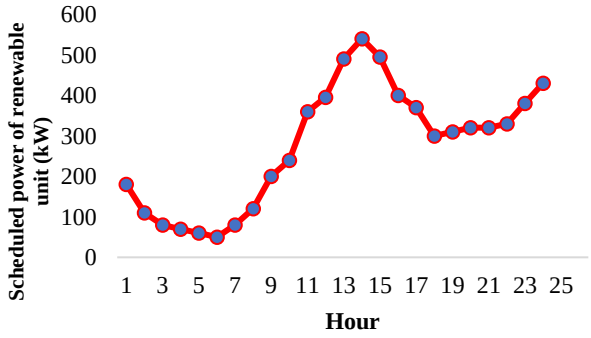

Fig.4. Predicted production capacity of non-dispatchable units in EC3

The simulations were performed using the CPLEX calculator in the GAMS software environment using an Intel(R) Xeon(R) E5-1630 v4@3.70 GHz processor and 16 GB of RAM. On this network, five ECs are assumed to exchange energy with each other. Each EC includes distributable (controllable power plant types) and non-distributable (wind and solar turbine) energy production units, adjustable loads, fixed loads, and an energy storage system. The simulation time horizon is also considered to be 24 hours. ECs are located on buses 20, 33, 40, 50, and 62 of the 69-bus distribution network and exchange energy with each other.

To execute the ADMM algorithm, all penalty parameters are set to 1, all initial values are set to zero, and the convergence criterion is set to 10^{-4}[29].

In the proposed method of this paper, in order to increase the flexibility in the network, feasible transaction regions are calculated considering the uncertainty of distributed generation units located in ECs and their agreement with the DSO, which causes energy exchanges to be established according to the maximum allowed capacity of ECs, which increases the volume of exchanges and brings more profit to the units along with maintaining the integrity of the network. This is while the limit of allowed exchanges in the network is traditionally calculated by the distribution network operator as dynamic operation envelopes and communicated to ECs, or these restrictions are applied as a fixed threshold during the exchange process. Figure 6 shows the real power peer-to-peer exchanges in a 24-hour period between 5 ECs using the proposed method based on calculating FTRs in the network. As is clear from the figure, ECs 3 and 5 are in the energy purchase position and ECs 1, 2 and 4 are in the energy sale position. Similarly, the reactive power exchanges of the ECs are also shown in Figure 7 according to the proposed method. As shown in Figure 7, in the reactive power exchanges, ECs 3, 4 and 5 are in the buying position and ECs 1 and 2 are mainly sellers.

In order to show the optimization process of the problem based on the calculation of FTRs, Figure 8 shows the convergence curve of the ADMM algorithm. By observing this figure, it is clear that the optimization problem has reached convergence after 130 iterations, which is acceptable, and the optimization has been carried out correctly and in the appropriate number of iterations, and the condition of reaching the optimal point has also been met.

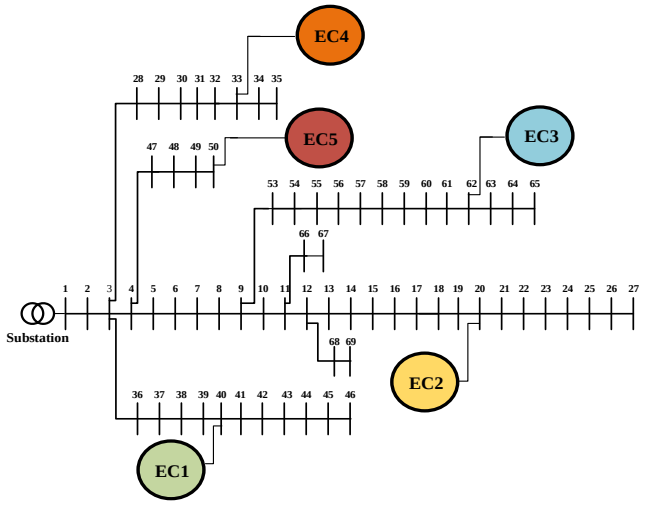

Fig. 5. Standard 69 bus network with 5 ECs.

Table 3. Technical characteristics of ECs (all in p.u.)

EC	$\left(\underline{P}_u^D, \overline{P}_u^D\right)$	$\left(\underline{Q}_u^D, \overline{Q}_u^D\right)$	R_u^D	$\left(\underline{P}_{v,t}^{ND}, \overline{P}_{v,t}^{ND}\right)$	$\left(\underline{P}_f^{FL}, \overline{P}_f^{FL}\right)$	E_f^{min}	$\left(\underline{P}_s^{ch,dch}, \overline{P}_s^{ch,dch}\right)$	$\left(\underline{E}_s, \overline{E}_s\right)$
EC1	(0,0.60)	(0,0.60)	0.15	(0.057,0.744)	(0.585,1.35)	18	(0,0.24)	(0.60,3)
EC2	(0,0.60)	(0,0.60)	0.15	(0.129,1.734)	(0.53,1.237)	12	(0,0.24)	(0.60,3)
EC3	(0,0.60)	(0,0.60)	0.15	(0.399,5.304)	(0.455,1.05)	9	(0,0.24)	(0.60,3)
EC4	(0,0.60)	(0,0.60)	0.15	(0.111,1.485)	(0.39,0.90)	13.5	(0,0.24)	(0.60,3)
EC5	(0,0.60)	(0,0.60)	0.15	(0.279,3.714)	(0.216,0.50)	3	(0,0.24)	(0.60,3)

Table 4. Economic characteristics of ECs

Prosumer	$\gamma_{u,t}^D\left(\$/p.u.\right)$	$\gamma_{v,t}^{ND}\left(\$/p.u.^2\right)$	$\gamma_{f,t}^{FL}\left(\$/p.u.^2\right)$	$\gamma_{s,t}^{Deg}\left(\$/p.u.^2\right)$	Location (bus)
EC1	2.7	160	100	4	(40)
EC2	5.2	160	900	4	(20)
EC3	5.8	160	400	4	(62)
EC4	2.54	160	625	4	(33)
EC5	2	160	400	4	(50)

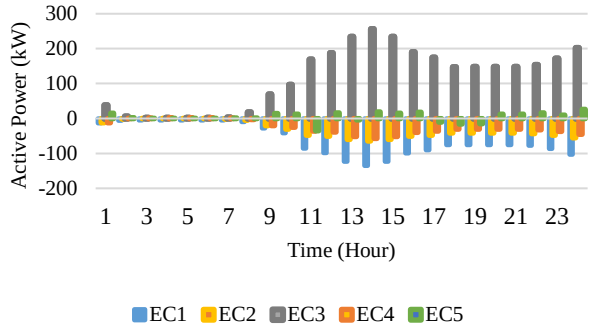

Fig. 6. P2P active power transactions of ECs according to the proposed method based on FTR calculation.

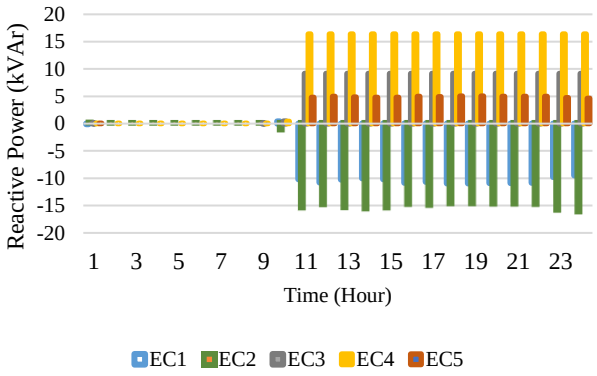

Fig. 7. P2P reactive power transactions of ECs according to the proposed method based on FTR calculation.

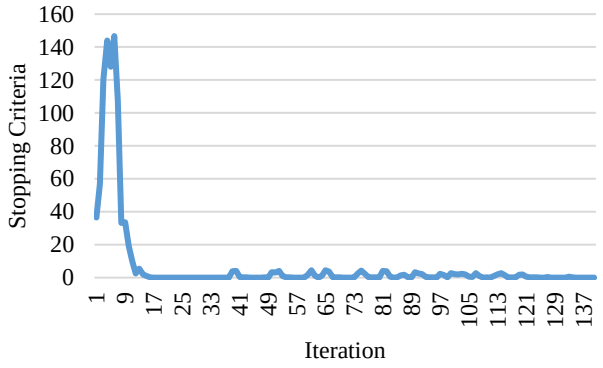

Fig. 8. The convergence curve of the ADMM algorithm in calculating the FTRs

5.2. Voltage Profile Investigation

In order to demonstrate the effectiveness of the proposed method in maintaining the network constraints within the permissible range, the average network voltage profile during peer-to-peer exchanges between ECs is presented in Figure 9. It can be seen that the permissible voltage range, which is a minimum of 0.95 and a maximum of 1.05 per unit [30], is observed during the exchanges, considering the energy exchange of the ECs within the calculated FTRs.

It should be noted that the voltage profile in other methods based on SOE and DOE is also within the permissible range because the operating region of ECs in those methods is determined and communicated to them by DSO.

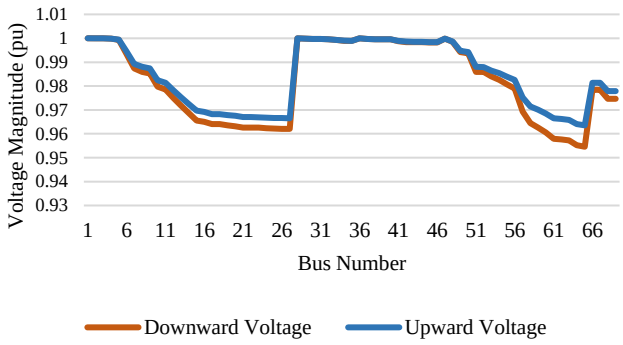

Fig. 9. Voltage profile of distribution network during P2P energy trading between ECs based on FTR calculation in the proposed method

5.3. Uncertainty evaluation of ECs by calculating different confidence levels

One of the criteria for validating the proposed method based on FTR is to investigate different confidence levels in the production units of ECs. In the proposed method, the variable δ, described in relations 33 - 38, shows the inherent uncertainty of distributed generation resources located in ECs. By changing this parameter, the production range of ECs changes and, as a result, the feasible transaction regions also change. This is while in conventional methods based on SOE and DOE, where the operation range is communicated to ECs by DSO, the inherent uncertainty of energy generation resources is not considered in the trades and determination of operation regions. This causes reduction in the volume of energy exchanges in the network and also cause the need for flexibility to establish technical network restrictions. In Figure 10, for example, the feasible transaction regions based on different confidence levels (δ = 0.5, 0.75) for EC1 has been calculated. The operation area has also been calculated and displayed using the DOE method. According to Figure 10, it can be seen that in the proposed FTR-based method, the preferences of ECs are considered in determining the permissible operation limits, and these preferences change with the parameter δ, which increases the incentive for ECs to participate in P2P transactions in local electricity markets and increases the volume of exchanges, while in the DOE-based method, such a parameter is not considered.

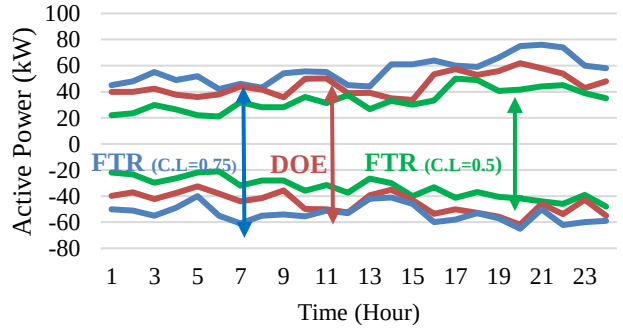

Fig. 10. Comparison of proposed FTR method based on confidence level=0.5, 0.75 and DOE method in calculating operation envelopes.

5.4. The effect of the proposed method on the volume of energy transactions

In order to demonstrate the effectiveness of the proposed method in terms of increasing the volume of exchanges in the network, the method proposed in this paper in determining the feasible transaction regions of ECs has been compared with two conventional methods of non-agreement dynamic operational envelopes with ECs [20] and static operational envelopes [19] for real and reactive power peer-to-peer exchanges. It should be noted that all three methods are

successful in terms of maintaining the technical constraints of the network within the permissible range. Table 5 presents the 24-hour volume of real and reactive power exchange between 5 ECs by the 3 methods mentioned, which shows that the proposed method has a 43.3% increase in exchanges compared to the method of applying static operational envelopes and a 20% increase in exchanges compared to the method based on DOE method. Also, the volume of reactive power exchanges in the proposed method has a growth of 49% compared to the method of static operational envelopes and 23% compared to the DOE method. The proposed method takes into account the inherent uncertainties of distributed generation resources located in ECs, allows for more accurate planning of ECs, and also uses their maximum capacity in the local electricity market. While in SOE and DOE methods, operating envelopes are imposed unilaterally by DSO, which causes the ECs' preferences not to be considered and, as a result, their maximum operating capacity are not used.

5.5. Total Cost of ECs

One of the important indicators for comparing the proposed method with other methods is the cost of ECs during peer-to-peer energy exchanges. This index has been simulated and compared for five ECs using the proposed method and another conventional method in determining the permitted area of ECs' transactions. Table 6 shows the results of the total cost of P2P trades of ECs, using different methods (Equation 1). According to the obtained results, it is observed that the total cost of ECs has been reduced in the proposed method compared to other methods. This cost reduction in itself increases the volume of transactions in the proposed method compared to other methods, which can also be seen in the results of table 5.

Table 5. Comparison of the proposed method with two methods based on applying technical constraints regarding the volume of P2P transactions within a 24-hour timeframe

Reference	Network Constraint Modeling	Active Power Trading Volume (kW)	Reactive Power Trading Volume (kVar)
[10]	SOE	3440	61
[20]	DOE	4110	74
Proposed method	FTR	4930	91

Table 6. Comparison of the total cost of ECs during a 24h P2P energy trading based on the proposed FTR method, base case, SOE and DOE methods.

Method	Total Cost ($)	Total Cost Reduction (%)
Base Case	1280	-
SOE	1190	7
DOE	1096	14.4
FTR	1051	17.8

5.6. Active and Reactive Power Losses

To demonstrate the performance of the proposed method in the real and reactive power loss index, the simulation results of the proposed FTR method, DOE method, SOE method and the base case are shown in Table 7. The results show that the peer-to-peer energy trading with the proposed method have reduced active losses by 19.35% and reactive losses by 22% compared to the base case. In the simulation with the DOE method, the active and reactive losses have been reduced by 14/8 and 14.3% respectively compared to the base case, and also in the simulation with the SOE method, the active and reactive losses have been reduced by 6.5 and 5.8% respectively compared to the base case.

Therefore, the proposed method provides a more appropriate performance in reducing real and reactive losses than other conventional methods.

Table 7. Power losses based on proposed FTR method compared with the base case, SOE and DOE method

Method	Rective Power Losses Reduction (%)	Rective Power Losses (kVar)	Active Power Losses Reduction (%)	Active Power Losses (kW)
Base Case	-	1351	-	2929
SOE	5/8	1272	6/5	2740
DOE	14/3	1158	14/8	2495
FTR	22	1054	19/35	2362

5. Conclusions

In this paper, a peer-to-peer exchange framework between ECs in an active distribution network is presented, in which, to increase flexibility in the network and use the maximum capacity of distributed generation resources, the permissible operating limits of the network are maintained by calculating an area called feasible transaction regions (FTRs). This permissible operating area is calculated from the agreement between the distribution system operator and energy communities and is not communicated unilaterally by the distribution network operator, as in previous studies. This point causes the ECs to share the operating limits with the distribution network operator, considering their uncertainty, inherent uncertainty, and required flexibility, and as a result, the permissible operating area presented in this paper is calculated bilaterally and is welcomed by the producers. This method has been implemented on a standard 69-bus network and the results show that, in addition to maintaining the technical constraints desired by the distribution network operator during exchanges, the volume of exchanges between local producers, which in this paper are energy communities, has increased compared to previous methods, which can increase flexibility in the network and also increase the motivation of subscribers to participate in local electricity markets based on peer-to-peer energy exchanges. In addition, this study, by calculating different confidence levels in determining the uncertainty of ECs, shows the effect of considering the permissible operating threshold in agreement with the network operator in the proposed method compared to other conventional methods. In the proposed structure, all ECs solve their optimization problems in parallel. Consequently, the time required to execute each iteration of the algorithm equals the sum of the maximum solution time among the ECs and the solution time for the DSO's problem. Based on this, the total solution time is 42.4 seconds. Given that the market is cleared one day ahead of the operating day, this computational burden does not pose a complexity issue.

References

[1] K. Taghizad-Tavana, M. Ghanbari-Ghalehjoughi, A. Safari, M. T. Hagh, and A. E. Nezhad, "From green hydrogen production to artificial intelligence–driven energy management in hydrogen fuel cell electric vehicles: a comprehensive review of technologies, optimization techniques, international standards, and investment programs", *Applied Energy*, vol. 399, p. 126534, 2025.

[2] T. Capper, A. Gorbatcheva, A. Mustafa, M. Bahloul, J. M. Schwidtal, R. Chitchyan, M. Andoni, V. Robu, M. Montakhabi, I. j. Scott, C. Francis, T. Mbavarira, J. M. Espana, L. Kiesling, "Peer-to-peer, community self-consumption, and transactive energy: A systematic literature review of local energy market models", *Renewable and Sustainable Energy Reviews*, vol. 162, p. 112403, 2022.

[3] B. Ahmadisourenabadi, M. Marzband, S. Hosseini-Hemati, S. M. B. Sadati, and A. Rastgou, "Quantifying and enabling the resiliency of a microgrid considering electric vehicles using a Bayesian network risk assessment", *Energy*, vol. 308, p. 133036, 2024.

[4] S. Deshmukh, H. Tariq, M. Amir, A. Iqbal, M. Marzband, and A. M. Al-Wahedi, "Impact Assessment of Electric Vehicles Integration and Optimal Charging Schemes Under Uncertainty: A Case Study of Qatar", *IEEE Access*, vol. 12, pp. 131350-131371, 2024.

[5] A. Alhendi, A. S. Al-Sumaiti, M. Marzband, R. Kumar, and A. A. Z. Diab, "Short-term load and price forecasting using artificial neural network with enhanced Markov chain for ISO New England", *Energy Reports*, vol. 9, pp. 4799–4815, 2023.

[6] M. S. Jonban, L. Romeral, M. Marzband, and A. Abusorrah, "Intelligent fault tolerant energy management system using first-price sealed-bid algorithm for microgrids", *Sustainable Energy, Grids and Networks*, vol. 38, p. 101309, 2024.

[7] M. S. Jonban, L. Romeral, M. Marzband, and A. Abusorrah, "A reinforcement learning approach using Markov decision processes for battery energy storage control within a smart contract framework", *Journal of Energy Storage*, vol. 86, p. 111342, 2024.

[8] J. Hossain, N. Saeed, R. Manojkumar, M. Marzband, K. Sedraoui, and Y. Al-Turki, "Optimal peak-shaving for dynamic demand response in smart Malaysian commercial buildings utilizing an efficient PV-BES system", *Sustainable Cities and Society*, vol. 101, p. 105107, 2024.

[9] A. Salari, M. Zeinali, and M. Marzband, "Model-free reinforcement learning-based energy management for plug-in electric vehicles in a cooperative multi-agent home microgrid with consideration of travel behavior", *Energy*, vol. 288, p. 129725, 2024.

[10] M. A. Mirzaei, K. Zare, B. Mohammadi-Ivatloo, M. Marzband, and A. Anvari-Moghaddam, "Techno-economic, environmental and risk analysis of coordinated electricity distribution and district heating networks with flexible energy resources", *IET Renewable Power Generation*, vol. 17, no. 12, pp. 2935–2949, 2023.

[11] S. Y. Rahme, S. Islam, S. M. Amrr, A. Iqbal, I. Khan, and M. Marzband, "Adaptive sliding mode control for instability compensation in DC microgrids due to EV charging infrastructure", *Sustainable Energy, Grids and Networks*, vol. 35, p. 101119, 2023.

[12] J. Guerrero, A. C. Chapman, and G. Verbič, "Decentralized P2P energy trading under network constraints in a low-voltage network", *IEEE Transactions on Smart Grid*, vol. 10, no. 5, pp. 5163-5173, 2018.

[13] J. Guerrero, B. Sok, A. C. Chapman, and G. Verbič, "Electrical distance driven peer-to-peer energy trading in a low-voltage network*", Applied Energy*, vol. 287, p. 116598, 2021.

[14] H. J. Kim, Y. S. Chung, S. J. Kim, H. T. Kim, Y. G. Jin, and Y. T. Yoon, "Pricing mechanisms for peer-to-peer energy trading: Towards an integrated understanding of energy and network service pricing mechanisms", *Renewable and Sustainable Energy Reviews*, vol. 183, p. 113435, 2023.

[15] A. Paudel, L. P. M. I. Sampath, J. Yang, and H. B. Gooi, "Peer-to-peer energy trading in smart grid considering power losses and network fees", *IEEE Transactions on Smart Grid*, vol. 11, no. 6, pp. 4727-4737, 2020.

[16] Z. Guo, P. Pinson, S. Chen, Q. Yang and Z. Yang, "Chance-constrained peer-to-peer joint energy and reserve market considering renewable generation uncertainty", *IEEE Transactions on Smart Grid*, vol. 12, no. 1, pp. 798-809, 2021.

[17] M. Z. Golambahri, M. Shakarami, and M. Doostizadeh, "Security-aware joint energy and flexibility trading in electricity-heat networks: A novel clearing and validation analysis", *International Journal of Electrical Power & Energy Systems*, vol. 157, p. 109901, 2024.

[18] R. Rezvanfar, K. Taghizad-Tavana, and M. T. Hagh, "A Comprehensive Review and Simulation-Based Analysis of Power Market Pricing Mechanisms in Energy Systems with High Penetration of Distributed Energy Resources: An Analysis of Distribution Locational Marginal Pricing, Dynamic Tariff, and Machine Learning-Based Approaches", *e-Prime-Advances in Electrical Engineering, Electronics and Energy*, p. 101083, 2025.

[19] M. I. Azim, W. Tushar, and T. K. Saha, "Coalition graph game-based P2P energy trading with local voltage management", *IEEE transactions on smart grid*, vol. 12, no. 5, pp. 4389-4402, 2021.

[20] A. Koirala, F. Geth, and T. Van Acker, "Day-ahead dynamic operating envelopes using stochastic unbalanced optimal power flow", *Sustainable Energy, Grids and Networks*, vol. 40, p. 101528, 2024.

[21] G. Lankeshwara and R. Sharma, "Dynamic operating envelopes-enabled demand response in low-voltage residential networks", in *2022 IEEE PES 14th Asia-Pacific Power and Energy Engineering Conference (APPEEC)*, pp. 1-7, 2022.

[22] T. Milford and O. Krause, "Managing DER in distribution networks using state estimation & dynamic operating envelopes", in *2021 IEEE PES Innovative Smart Grid Technologies-Asia (ISGT Asia)*, pp. 1–5, 2021.

[23] M. R. Alam, P. T. Nguyen, L. Naranpanawe, T. K. Saha, and G. Lankeshwara, "Allocation of dynamic operating envelopes in distribution networks: Technical and equitable perspectives", *IEEE Transactions on Sustainable Energy*, vol. 15, no. 1, pp. 173–186, 2023.

[24] Z. Jiang, Y. Guo, and J. Wang, "Dynamic operating envelopes embedded peer-to-peer-to-grid energy trading", *Applied Energy*, vol. 377, p. 124554, 2025.

[25] H. Zhu, Y. Gao, and Y. Hou, "Real-Time Pricing for Demand Response in Smart Grid Based on Alternating Direction Method of Multipliers", *Mathematical Problems in Engineering*, vol. 2018, no. 1, p. 8760575, 2018.

[26] L. Chen, S. He, and X. Fan, "Cooperative optimization of shared energy storage in integrated energy systems using adaptive ADMM and Nash bargaining", *Journal of Energy Storage*, vol. 134, p. 118148, 2025.

[27] S. Feng, W. Wei, and Y. Chen, "Day-ahead scheduling and online dispatch of energy hubs: A flexibility envelope approach", *IEEE Transactions on Smart Grid*, vol. 15, no. 3, pp. 2723-2737, 2023.

[28] S. P. Boyd and L. Vandenberghe, "Convex optimization", Cambridge university press, 2004.

[29] K. Subbaramaiah and P. Sujatha, "Optimal DG unit placement in distribution networks by multi-objective whale optimization algorithm & its techno-economic analysis", *Electric Power Systems Research*, vol. 214, p. 108869, 2023.

[30] T. Hai, N. S. S. Singh, and F. Jamal, "Energy management of a microgrid with integration of renewable energy sources considering energy storage systems with electricity price", *Journal of Energy Storage*, vol. 110, p. 115191, 2025.